ANALYSIS OF INCREASING THE FRICTION FORCE OF THE ROBOT JAWS BY ADDING 3D PRINTED FLEXIBLE INSERTS

JIRI SUDER, TOMAS KOT, ALAN PANEC*, MICHAL VOCETKA

VSB - Technical University of Ostrava, Department of Robotics,
* Institute of Physical Education and Sports, Ostrava,
Czech Republic

DOI: 10.17973/MMSJ.2021_12_2021127

jiri.suder@vsb.cz

3D printing technology plays a key role in the production of prototypes and final functional parts. The ability to produce almost any shape using this technology in combination with lightweight materials is often used to minimise the weight of the designed components. However, for some applications, such as robot gripper jaws, conventional most commonly used materials, such as PLA, may be unsuitable due to their low coefficient of friction on the material of the manipulated object, which in some cases may cause the object to slip in the robot jaws. This article describes a technical problem from practice, where a manipulated object made of steel material slipped in the printed PLA jaws of the robot during its working cycle. This work is devoted to increasing the friction force of the robot jaws by adding 3D printed soft inserts. Two insert surface shapes made of two flexible materials TPU 30D and TPE 88 are tested. The increase in friction force is measured on a measuring device with an industrial robot and a force measuring sensor. The most suitable type of inserts and material is then tested on a collaborative robot at its required working cycle. The results of this experiment are intended to help designers as a source of information or inspiration in designing similar applications.

KEYWORDS

Fused Filament Fabrication, 3D Print, Flexible Filament, Friction, Robotic Gripping, Jaw

1 INTRODUCTION

3D printing technology plays a key role in the production of prototypes and final functional parts [Suder 2021]. It allows to create shapes that would not be possible to produce with other known technologies, or their production would be too expensive or time-consuming [Beniak 2020]. The possibility of producing almost any shape in combination with light materials is often used in robotics, such as cover for a snake robot [Virgala 2021], robotics vehicle [Pastor 2017], topology optimized robotic arms [Paska 2020], flexible wheels of mobile robots [Pastor 2020], end effectors for calibration [Huczala 2020], or for printing robotic jaws [Suder 2018].

Robot jaws can be made of either classic hard material (in some cases it may be desirable to measure the gripping force to avoid damage to the manipulation object [Suder 2018][Kot 2017], or soft materials for adaptive gripping [Suder J. 2021], or a combination thereof. In robotics, it is suitable to design the jaws so that they are soft enough at the area of contact with the object of manipulation so as not to damage the surface of the gripped object. At the same time, it is advantageous to increase the coefficient of friction as much as possible. By increasing the coefficient of friction, smaller gripping force is sufficient to derive the required frictional force, which may eventually mean using a less powerful and lighter drive, which can reduce the overall weight of the structure and energy requirements for the system operation [Zeman 2021].

This article deals with research based on practical requirements [Vocetka 2020], where it was necessary to ensure a minimum weight of the jaws on the YuMi collaborative robot [ABB 2021]. This robot has a load capacity of 500 g [ABBGripper 2021], which includes the object of manipulation and the end effector. The object of handling is a DC motor weighing 273 g. However, due to the weight of the used pneumatic gripper (203 g), the weight available for two jaws is only 24 g, i.e. 12 g per one jaw. The requirement for this low jaw weight led to the use of 3D printing, and its shape was generated by topological optimisation [Vocetka 2020]. The material of the original jaw is PLA [Prusament 2021]. This material has a relatively good tensile strength, which is approximately 46 MPa [Suder 2020], but it is limited by the relatively low glass transition temperature, which is approximately 60 °C [Suder 2021]. During the required movements of the robot in real testing, the object of manipulation (motor) slipped out of the jaw. The trajectories of the robot movements have been optimised according to two requirements, namely to minimise energy consumption [Vysocky 2020] and to minimise robot wear [Kot 2021]. For this reason, it was no longer appropriate to change this trajectory. This experiment aimed to prevent the motor from slipping out of the jaw, which was ensured by inserting flexible inserts into the jaw. The jaw has been modified so that 3 printed inserts of soft material are inserted into it. The designed shape of the jaws and inserts is suitably adapted so that the inserts can be easily and quickly replaced in case of wear. The inserts should adapt more to the shape of the motor after gripping the motor, and its material should increase the friction coefficient. The original jaw weighs 10.15 g, and the modified jaw with inserted flexible inserts weighs 10.5 g. The requirement for maximum weight is therefore reached. Figure 1 shows the original jaw and the modified jaw.

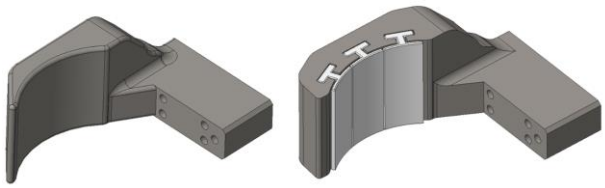

Figure 1. Left: original design, right: modified jaw with inserted flexible inserts

A measuring device with an industrial robot and a force measuring sensor was used to measure the increase in friction force. Two types of insert shapes and two types of materials, TPU 30D [Fiberlogy 2021] and TPE 88 [RubberJet 2021], were tested.

The work was performed on a measuring device that measures the increase in friction force for two types of materials and shapes of flexible inserts. After evaluating the most suitable shape and material, the jaws with flexible inserts were tested on a real collaborative robot during its required movement.

The results of this work can help designers as inspiration or a source of information in designing similar applications.

2 METHODOLOGY

For experimental analyses of the increase in friction force, inserts of flexible filaments and jaws were printed. The measuring device measured the force required to pull the manipulation object out of the jaws.

2.1 *Printed soft inserts*

Two variants of the shape of the inserts were chosen for testing, namely smooth inserts, and knurled inserts. Figure 2 shows the shapes of these inserts.

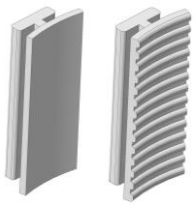

Figure 2. Left: smooth insert, right: knurled insert

Two soft materials were tested. The first material is TPU 30D [Fiberlogy 2021] and the second material is TPE 88 [RubberJet 2021]. The coefficient of friction of these materials is higher than the coefficient of PLA, but the exact value to the material of the motor cover is not specified by the manufacturer [Fiberlogy 2021] [RubberJet 2021].

The jaws were printed on the Original Prusa i3 MK3S 3D printer [Prusa 2021]. All inserts were printed on the Original Prusa i3 MK3S 3D printer with the Flexion extruder [Flexion 2021], installed, specially designed for printing from flexible filaments. The jaws themselves were printed on a printer with an original extruder. For the data conversion from 3D models to G-codes for the printer, the program PrusaSlicer 2.3.0 [PrusaSlicer 2021] was used.
The selection of the most important printing parameters is shown in Table 1.

Parameter	Value
Filament diameter	1.75 mm
Nozzle diameter	0.4 mm
Layer height	0.2 mm
Infill	100 %
Nozzle temperature for material PLA	215 °C
Nozzle temperature for flexible materials	210 °C
Bed temperature	60 °C
Number of perimeters	2
Perimeter speed	45 mm/s
Speed for infill	80 mm/s
Speed for first layer	20 mm/s
Speed for top layer	40 mm/s

Table 1. The used basic printing parameters

2.2 *Measuring of friction force*

An ABB IRB 1600 industrial robot [IRB1600 2021] with an ABB Small force sensor [Robotics 2021] was used for measurement. This assembly measures the magnitude of the force up to 495 N with an accuracy of 0.11 N and a positioning accuracy of 0.02 mm [IRB1600 2021] [Robotics 2021]. Before the measurement itself, the industrial robot performed its work cycle for 2 hours to warm it up to the operating temperature and thus maximise the repeatable positioning accuracy of the robot [Vocetka M. 2020]. The measurement system is shown in Figure 3.

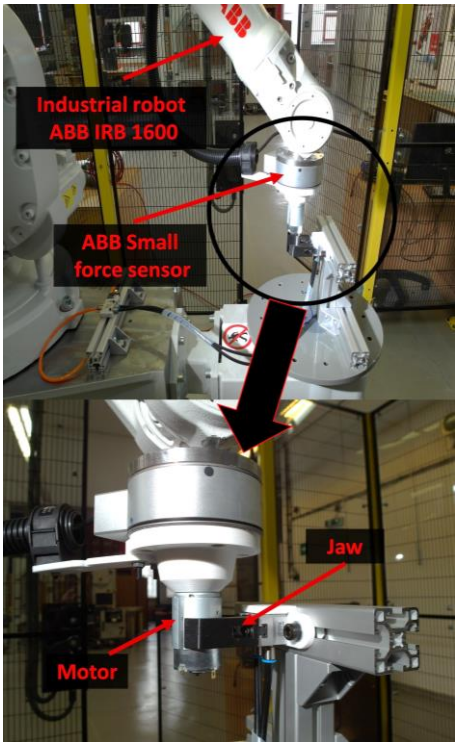

Figure 3. Measurement system, top: the whole system, bottom: detailed view of the jaw

The motor is rigidly attached to the flange of the robot, on which the ABB Small force sensor for measuring the force is mounted. The jaws are screwed to the pneumatic gripper [Festo 2021]. At the starting position for the measurement, the DC motor is located in the middle of the open jaws. The gripper is fully open, and the axis of the DC motor is in the middle of the gripper. After setting the required gripper pressure, the jaws grip the DC motor. The measuring is performed for 3 gripper pressures 0.3, 0.6 and 0.8 MPa, which according to the catalogue of the gripper manufacturer [Festo 2021] corresponds to the magnitude of the gripping force 15, 35 and 50 N per jaw. Subsequently, the robot moves only in the direction of the motor axis at a constant speed of 10 mm/s. The force sensor records the amount of force required to pull the motor out of the jaw grip. The whole procedure is repeated for the jaws with the inserts.
The force distribution diagram is shown in Figure 4.

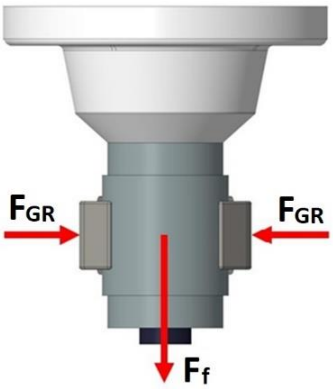

Figure 4. The force distribution diagram

According to Figure 4, the coefficient of shear friction is calculated according to the following formula.

$$F_f = 2 \cdot F_{GR} \cdot \mu \rightarrow \mu = \frac{F_f}{2 \cdot F_{GR}} \quad (1)$$

Where F_t is the friction force, F_{GR} is the gripping force, and μ is the coefficient of shear friction.

3 RESULTS

The results consist of measured values and testing performed on a real device.

3.1 Measured data

Figure 5 shows the selected diagrams of measured friction forces for individual gripping forces depending on the jaws used.

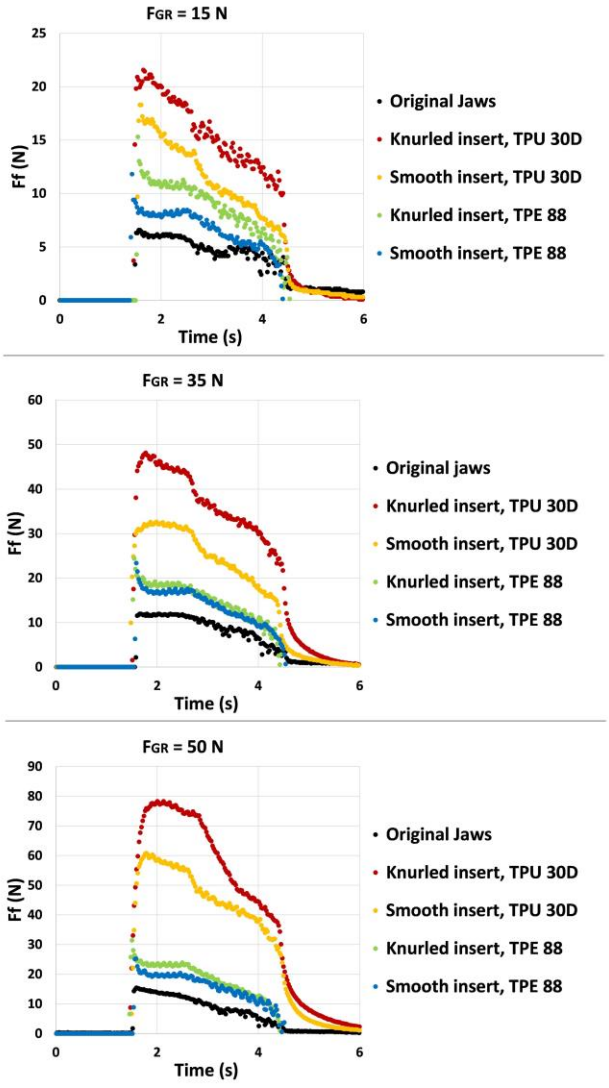

Figure 5. Measured force diagram. Top: for gripping force 15 N, middle: for gripping force 30 N, bottom: for gripping force 50 N

The measurement confirmed the increase in the friction force required to pull the motor after using the flexible inserts, this force increased depending on the type of inserts used, their material, and the magnitude of the gripping force. Table 2 shows the maximum measured values of friction forces for individual jaws and gripping forces.

Jaws	F_f (N)		
	F_{GR} (N)	F_{GR} (N)	F_{GR} (N)
	15	35	50
Original jaws	6.40 ± 0.28	11.71± 0.51	15.36 ± 0.50
Knurled inserts, TPU 30D	21.48 ± 0.45	48.10 ± 0.53	78.56 ± 0.54
Smooth inserts, TPU 30D	18.37 ± 0.33	32.26 ± 0.48	60.44 ± 0.46
Knurled inserts, TPE 88	15.38 ± 0.42	24.42 ± 0.50	31.44 ± 0.71
Smooth inserts, TPE 88	11.67 ± 0.49	23.52 ± 0.41	25.30 ± 0.61

Table 2. Measured values of friction forces for tested samples

Figure 6 shows a statistical evaluation of the measured friction forces for the individual gripping forces, the tested jaws and the materials.

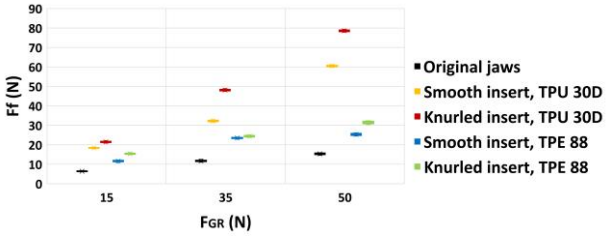

Figure 6. Box plot of friction force - gripping force dependence for test specimens

From Figure 6, it can be seen that a higher frictional force was measured for all inserts compared to the original jaws. The most significant increase in friction force is in the jaws with inserts made of the TPU 30D material. In terms of the surface of these inserts, higher values of frictional forces were measured for knurled inserts than for smooth inserts.

The percentage increase in frictional force when using inserts compared to the original magnitude of the measured force is shown in Table 3.

Jaws	Percentage increase in F_f (%)		
	F_{GR} (N)	F_{GR} (N)	F_{GR} (N)
	15	35	50
Knurled inserts, TPU 30D	235.63	310.62	411.46
Smooth inserts, TPU 30D	187.09	175.40	293.49
Knurled inserts, TPE 88	140.34	108.47	104.69
Smooth inserts, TPE 88	82.28	100.79	64.71

Table 3. Percentage increase in force compared to the original jaws

According to Table 3, it is clear that the most significant percentage increase was achieved by the knurled inserts made of the TPU 30D material. This percentage increase depends on the magnitude of the gripping force.

From the measured values, the coefficients of shear friction were calculated according to formula (1). The coefficients of shear friction are shown in Table 4.

Jaws	Coefficient of shear friction μ (-)		
	F_{GR} (N)	F_{GR} (N)	F_{GR} (N)
	15	35	50
Original jaws	0.21 ± 0.01	0.17 ± 0.01	0.15 ± 0.01
Knurled inserts, TPU 30D	0.72 ± 0.02	0.69 ± 0.01	0.79 ± 0.01
Smooth inserts, TPU 30D	0.61 ± 0.01	0.46 ± 0.01	0.60 ± 0.01
Knurled inserts, TPE 88	0.51 ± 0.01	0.35 ± 0.01	0.31 ± 0.01
Smooth inserts, TPE 88	0.39 ± 0.05	0.34 ± 0.01	0.25 ± 0.01

Table 4. Coefficients of shear friction

The results in Table 4 show that the coefficient of shear friction increases to a value around 0.69 to 0.79 when the knurled inserts from the TPU 30D material were used. The magnitude of the coefficient of friction depends not only on the type of used inserts but also on the magnitude of the gripping force.

3.2 *Real testing on the collaborative robot YuMi*

Experiments have shown that using knurled inserts made of TPU 30D increases the frictional force (up to approximately 411%, depending on the magnitude of the gripping force). Subsequently, tests were performed on the YuMi robot at its required working cycle. Figure 7 shows a YuMi robot with jaws with knurled inserts from TPU 30D mounted on its "left" effector.

Figure 7. YuMi collaborative robot with a jaw with knurled inserts from TPU 30D

Even after 500 test cycles, there was not a single slip of the motor in the jaws. The designed inserts can thus be considered as a suitable solution for increasing the friction force and in this case also for ensuring contact between the jaws and the object of manipulation.

4 CONCLUSIONS

3D printing technology is used not only for rapid prototyping but also for final functional products. The advantages of this technology are commonly used with topological optimisation, which can rapidly reduce the weight of the manufactured part. A wide range of different materials, both hard and soft, is often used in robotics.

This work was based on practical requirements. Due to the low coefficient of shear friction, the object of manipulation slipped out of the jaws of the collaborative robot during its required movement. The work experimentally tested the effect of increasing the friction force, and thus the coefficient of shear friction after modification of the jaw, into which printed inserts made of soft materials were inserted. Two materials TPU 30D and TPE 88, and two types of inserts, were tested. The designed shape of the jaws and inserts is suitably adapted so that the inserts can be easily and quickly replaced in case of wear. The experiment was performed on a measuring system, which consisted of an industrial robot and a force sensor. The object of manipulation was gripped with a specified force into the jaws, which were firmly connected to the ground. The industrial robot pulled this manipulation object from the jaws, measuring the frictional force required to pull the object.

The experiments show that the use of flexible inserts made of TPU 30D material with a knurled surface increases the frictional force by up to approximately 411%. However, the magnitude of this increase depends on the magnitude of the gripping force. The smallest increase occurs with the material TPE 88. While the coefficient of shear friction of the original jaws reached values around 0.15 to 0.21 (depending on the magnitude of the gripping force), the knurled inserts made of TPU 30D increased this coefficient by around 0.69 to 0.79. It is clear from the measurements that the magnitude of the coefficient of shear friction depends not only on the inserts used but also on the magnitude of the gripping force. According to the test results, the most suitable inserts were selected, which were tested on a collaborative robot during its required work cycle. Even after 500 cycles, there was no slip in any case, which verified the correctness of the solution.

The results of this work can help designers as inspiration or a source of information in designing similar applications.

ACKNOWLEDGMENTS

This article has been elaborated under support of the project Research Centre of Advanced Mechatronic Systems, reg. no. CZ.02.1.01/0.0/0.0/16_019/0000867 in the frame of the Operational Program Research, Development and Education. This article has been also supported by specific research project SP2021/47 and financed by the state budget of the Czech Republic.

REFERENCES

[ABB 2021] ABB. IRB 14 000 YuMi. ABB, 2021, [online]. Available from https://new.abb.com/products/robotics/cs/kolaborativni-roboty/yumi?utm_source=google&utm_campaign=SE_Roboty_Roboty&utm_medium=cpc&utm_term=Roboty&utm_content=Robot-YUMI&gclid=EAIaIQobChMItqTrrJ-O4QIVQZztCh06BAyrEAAYASAAEgJVovD_BwE

[ABBGripper 2021] ABBGripper. Productmanual IRB 14000 gripper. ABB, 2021, [online]. Available from https://abb.sluzba.cz/Pages/Public/IRC5RoboticsDocumentationRW6/Robots/Collaborative%20Robots/en/3HAC054949-001.pdf

[Beniak 2020] Beniak, J., et al. Strength produced parts by fused deposition modeling. Global Journal of Engineering and Technology Advances, 2020, Vol. 5, pp 57-62, ISSN 1803-1269, doi: 10.30574/gjeta.2020.5.2.0101

[Festo 2021] Festo. Parallel gripper HGPT-16-A-B. FESTO, 2021, [online]. Available from https://www.festo.com/cat/xdki/data/doc_engb/PDF/EN/HGPT-B_EN.PDF

[Fiberlogy 2021] Fiberlogy. TECHNICAL DATA SHEET FIBERFLEX 30D, 2021, [online]. Available from https://www.materialpro3d.cz/user/related_files/tds_fiberflex_30d_en.pdf

[Flexion 2021] Single Flexion retrofit kit for single extruder. DIABASE, 2021, [online]. Available from https://flexionextruder.com/shop/single/

[Huczala 2020] Huczala, D., et al. Camera-Based Method for Identification of the Layout of a Robotic Workcell. Applied Sciences. Vol. 10, No.21, 2020, pp 1-14, ISSN 2076-3417, doi: 10.3390/app10217679

[IRB1600 2021] IRB1600. Technical data for the IRB 1600 industrial robot. ABB, 2021, [online]. Available from https://www.prusa3d.com/prusaslicer/#_ga=2.96407198.300644305.1591643943-1493863876.1591643943

[Kot 2021] Kot, T., et al. Method for Robot Manipulator Joint Wear Reduction by Finding the Optimal Robot Placement in a Robotic Cell. Applied Sciences, 2021, Vol. 11, No. 5398, pp 1-19, ISSN 2076-3417, doi: 10.3390/app11125398

[Kot 2017] Kot, T., et al. Gripper with precisely adjustable gripping force. In Proceedings of the 18th International Carpathian Control Conference, ICCC 2017, 2017, pp 555-559, ISSN 978-1-5090-4862-5, doi: 10.1109/CarpathianCC.2017.7970462

[Paska 2020] Paska, Z., et al. METHODOLOGY OF ARM DESIGN FOR MOBILE ROBOT MANIPULATOR USING TOPOLOGICAL OPTIMIZATION. MM Science Journal, June 2020, Vol. 2020, No. March, March 2021, pp 3918-3925, ISSN 1803-1269, doi: 10.17973/MMSJ.2020_06_2020008

[Pastor 2020] Pastor, R., et al. Modular Rover Design for Exploration and Analytical Tasks. Modelling and Simulation for Autonomous Systems. Springer International Publishing. 2020, pp 203-215, ISSN 0302-2974, doi: 10.1007/978-3-030-43890-6_16

[Pastor 2017] Pastor, R., et al. Semi-autonomous robotic system for reconnaissance. 2017 IEEE 21st International Conference on Intelligent Engineering Systems (INES), October 2017, pp 119-124, doi: 10.1109/INES.2017.8118540

[Prusa 2021] Prusa. Original Prusa i3 MK3S+ 3D printer, 2021, [online]. Available from https://shop.prusa3d.com/en/3d-printers/181-original-prusa-i3-mk3s-3d-printer.html#

[Prusament 2021] Prusament. Prusament PLA Jet Black 1kg - Prusa Research, 2021, [online]. Available from https://shop.prusa3d.com/en/prusament/959-prusament-pla-jet-black-1kg.html

[PrusaSlicer 2021] PrusaSlicer. PrusaSlicer 2.3, 2021, [online]. Available from https://www.prusa3d.com/prusaslicer/#_ga=2.96407198.300644305.1591643943-1493863876.1591643943

[Robotics 2021] Robotics. Product manual Integrated Force Control. ABB, 2021, [online]. Available from https://abb.sluzba.cz/Pages/Public/IRC5RoboticsDocumentationRW6/Application%20Equipment%20&%20Accessories/Integrated%20Force%20Control/en/3HAC048488-001.pdf

[RubberJet 2021] RubberJet. TPE 88 RubberJet Flex. Filament PM, 2021, [online]. Available from https://www.filament-pm.cz/tpe-88-rubberjet-flex-translucent-1-75-mm-0-5-kg/p91?do=openSendToFriend

[Suder 2021] Suder, J., et al. EXPERIMENTAL ANALYSIS OF TEMPERATURE RESISTANCE OF 3D PRINTED PLA COMPONENTS. MM Science Journal, March 2021, Vol. 2021, No. March, pp 4322-4327, ISSN 1803-1269, doi: 10.17973/MMSJ.2021_03_2021004

[Suder J. 2021] Suder, J., et al. Structural Optimization Method of a FinRay Finger for the Best Wrapping of Object. Applied Sciences, 2021, Vol. 11, No. 3858, pp 1-18, ISSN 2076-3417, doi: 10.3390/app11093858

[Suder 2020] Suder, J., et al. VOCETKA. THE INFLUENCE OF ANNEALING TEMPERATURE ON TENSILE STRENGTH OF POLYLACTIC ACID. MM Science Journal, November 2020, Vol. 2020, No. November, pp 4132-4137, ISSN 1803-1269, doi: 10.17973/MMSJ.2020_11_2020048

[Suder 2018] Suder, J., et al. MODIFICATIONS TO THE EFFECTOR FOR MEASUREMENT OF GRIPPING FORCE. MM Science Journal, December 2018, Vol. 2018, No. December, pp 2606-2610, ISSN 1803-1269, doi: 10.17973/MMSJ.2018_12_2018100

[Virgala 2021] Virgala, I., et al. A snake robot for locomotion in a pipe using trapezium-like travelling wave. Mechanism and Machine Theory, Vol.158, 2021, pp 1-21, ISSN 0094-114X, doi: 10.1016/j.mechmachtheory.2020.104221

[Vocetka 2020] Vocetka, M., et al. DESIGN OF ALGORITHMS FOR AUTOMATIC SELECTION OF DRIVE UNITS FOR MECHATRONIC DEVICES. Acta Polytechnica, 2020, Vol. 60, No. 2, pp 4362-4370, ISSN 151–157, doi: https://doi.org/10.14311/AP.2020.60.0151

[Vocetka M. 2020] Vocetka, M., et al. Influence of the Approach Direction on the Repeatability of an Industrial Robot. Applied Sciences. Vol. 10, No.8714, 2020, pp 1-24, ISSN 2076-3417, doi: 10.3390/app10238714

[Vysocky 2020] Vysocky, A., et al. Reduction in Robotic Arm Energy Consumption by Particle Swarm Optimization. Applied Sciences, 2020, Vol. 10, No. 8241, pp 1-15, ISSN 2076-3417, doi: 10.3390/app10228241

[Zeman 2021] Zeman, Z., et al. DESIGN OF ALGORITHMS FOR AUTOMATIC SELECTION OF DRIVE UNITS FOR MECHATRONIC DEVICES. MM Science Journal, June 2021, Vol. 2021, No. June, pp 4362-4370, ISSN 1803-1269, doi: 10.17973/MMSJ.2021_6_2021011

CONTACTS:

Ing. Jiri Suder, Ph.D.
VSB - Technical University of Ostrava, Department of Robotics
17. listopadu 2172/15, Ostrava, 708 00, Czech Republic
+420 597 329 364, jiri.suder@vsb.cz, www.fs.vsb.cz/354